RESEARCH PAPER

Nitrogen-doped carbon dots as multifunctional fluorescent probes

**Fengyi Du · Xin Jin · Junhui Chen · Ye Hua · Mulan Cao · Lirong Zhang ·
Jianan Li · Li Zhang · Jie Jin · Chaoyang Wu · Aihua Gong · Wenrong Xu ·
Qixiang Shao · Miaomiao Zhang**

Abstract Highly fluorescent nitrogen-doped carbon dots (NCDs) were prepared through the hydrothermal carbonization of citric acid and ammonium acetate. The resulting NCDs were quasi-spherical particles with an average diameter of approximately 2.1 nm. They exhibited excellent photoluminescent properties and had favorable solubility in water. Furthermore, the NCDs had low cytotoxicity and were readily integrated with cytoplasm. This makes them particularly suitable for multicolor bioimaging. Most importantly, NCDs internalized by cancer cells can be detected at four channels simultaneously with flow cytometry, which further demonstrates that the NCDs can be used as multifunctional fluorescent probes for biomedical applications.

Keywords Carbon dots · Nitrogen-doped · Bioimaging · Flow cytometry

Fengyi Du, Xin Jin and Junhui Chen have contributed equally to this work.

F. Du (✉) · X. Jin · J. Chen · Y. Hua ·
L. Zhang · L. Zhang · J. Jin · C. Wu · A. Gong ·
W. Xu · Q. Shao · M. Zhang
School of Medicine, Jiangsu University,
Zhenjiang 212013, People's Republic of China
e-mail: biodfy@ujs.edu.cn; biodfy@qq.com

M. Zhang
e-mail: 278989547@qq.com

M. Cao
College of Biological and Chemical Engineering,
Panzhihua University, Panzhihua 617000,
People's Republic of China

J. Li
Department of Otolaryngology Head and Neck Surgery,
Chinese PLA General Hospital, Beijing 100853,
People's Republic of China

Introduction

Recently, carbon quantum dots (CDs), a new carbon-based nanomaterial, have attracted much attention because of their excellent properties and extensive applications in biomedical imaging (Cao et al. 2007; Li et al. 2012; Stefanakis et al. 2014), photocatalysis (Li et al. 2010), sensors (Liong et al. 2013), drug delivery (Wang et al. 2013), and optoelectronic devices (Guo et al. 2012). Fluorescent CDs were first discovered serendipitously by researchers who purified single-walled carbon nanotubes (SWCNTs) fabricated with the arc-discharge method (Xu et al. 2004). The CDs were discrete quasi-spherical nanoparticles with diameters smaller than 10 nm. CDs are generally composed of carbon, hydrogen, and oxygen in a quasi-spherical structure where the carbon shows the characteristics of crystalline graphite. In recent years, studies have verified that doping heteroatoms into CDs can effectively tune their intrinsic properties, as well as produce new phenomena and unexpected properties (Wei et al. 2014; Lai et al. 2013; Zhang et al. 2014; Jahan et al. 2013). Nitrogen atoms, which have a

comparable atomic size to carbon atoms and five valence electrons for bonding, have been widely used for doping CDs to create highly fluorescent CDs.

Approaches for synthesizing CDs can be classified into two main strategies: top-down and bottom-up methods. CDs produced with the top-down method are formed or broken off from large renewable resources, such as soy milk (Zhu et al. 2012), orange juice (Sahu et al. 2012), eggs (Wang et al. 2012), and cocoon silk (Li et al. 2013). Recently, our group demonstrated that renewable bagasse (sugarcane waste products) could be used as a new precursor to prepare fluorescent CDs (Du et al. 2014a). This method uses clean, cheap, and convenient starting materials to produce fluorescent CDs. Despite numerous achievements in this area, the complex chemical compositions and low fluorescence quantum yield of CDs when using top-down methods are still interesting challenges that inspire great interest. Conversely, CDs produced by bottom-up techniques are formed of small molecular precursors, including carbon-containing materials and passivation agents. The passivation agents always contain terminal NH_2 groups, such as amino-terminated polyethylene glycol (PEG) (Zhu et al. 2009), aqueous ammonia (Jiang et al. 2013), polyethylenimine (PEI) (Han et al. 2012), and 4,7,10-trioxa-1,13-tridecanediamine (TTDDA) (Zhai et al. 2012). The use of these passivation agents illustrated that nitrogen-containing groups acting as auxochromes could dramatically improve the photoluminescence (PL) of CDs. In addition, our previous work has demonstrated that the introduction of amino-containing groups into CDs can result in significantly accelerated polymerization and carbonization during the hydrothermal process (Du et al. 2014b). Currently, improving the fluorescent properties and broadening the applicability of CDs are the most popular research areas.

In our current study, we report a facile bottom-up route to synthesize fluorescent nitrogen-doped carbon dots (NCDs) through the hydrothermal carbonization of citric acid and ammonium acetate. Compared with previous papers, the as-prepared NCDs possess intense PL, favorable solubility in water, and stable optical properties. It is worth noting that heterogeneous multi-layered phase structures in NCDs have been observed for the first time. Most importantly, we have demonstrated that the good biocompatibility of the fabricated NCDs allows them to function as highly effective fluorescent probes for living cancer cells and imaging and labeling biomedical applications.

Materials and methods

Materials

Ammonium acetate, glucose, and quinine sulfate (98 %, suitable for fluorescence) were the product from sigma (New York, USA). 3-(4,5-Dimethyl-2-thiazoyl)-2,5-diphenyltetrazolium bromide (MTT, 98 %) was supplied by Alfa-Aesar (Beijing, China). Ammonia water, NaH_2PO_4, Na_2HPO_4, and H_2SO_4 were obtained from Guangfu Fine Chemical (Tianjin, China). Fetal bovine serum (FBS) and Dulbecco minimum essential medium (DMEM) medium were purchased from Invitrogen China Limited (China, Shanghai). And all of the chemicals were analytical reagent grade and were used without further purification.

Synthesis of NCDs

Firstly, certain amounts of citric acid and ammonium acetate were diluted with 20 ml water and under vigorous stirring to form a transparent homogeneous solution. Then, the solution was transferred into a microwave oven and heated for different times. When cooled down to room temperature, the black substance was dissolved and centrifuged at 5,000 rpm for 15 min to remove the black precipitates. The brown-yellow supernatant was dialyzed against ultra-pure water through a dialysis membrane (MWCO of 1,000) for 4 days to remove residues. The dialysis solution was collected and frozen dried by vacuum freeze dryer. Finally, the NCDs powers were obtained and saved for further characterization and application.

Instrumentation and characterizations

The chemical structure of NCDs was identified by Fourier transform infrared (FTIR) spectra (Nicolet Nexus 470, America). The elementary compositions were further confirmed by elemental analysis with CHNS-O Analyzer. The morphologies of the CDs were examined by high-resolution transmission electron microscopy (HRTEM) on a JEM-2100 microscope (Jeol, Japan) with an accelerating voltage of 200 kV. UV–vis absorption was characterized by UV-2450 UV–vis Spectrophotometer (Shimadzu, Japan). PL emission measurements were performed using Cary Eclipse Fluorometer (Varian, America).

The quantum yield (Φ) of the as-synthesized carbon nanodots was determined by a comparative method (Baker et al. 2010; Wang et al. 2012). As the standard measurement, the quinine sulfate (literature quantum yield: 54 %) was dissolved in 0.1 M H_2SO_4 [refractive index (η) = 1.33] and the NCDs were dissolved in distilled water (η = 1.33) at different concentrations. All the absorbance values of the solutions at the excitation wavelength were measured with UV–vis spectrophotometer. PL emission spectra of all the sample solutions were recorded by FLS920 fluorometer at an excitation wavelength of 360 nm. The samples were then measured by PL spectrometer in order to get the PL emission intensity at the excitation wavelength with which the NCDs and the reference have the same UV absorbance. Then the quantum yield was calculated by the following equation.

$$\Phi_X = \Phi_{st}\left(\frac{Grad_X}{Grad_{st}}\right)\left(\frac{\eta_X^2}{\eta_{st}^2}\right)$$

The ST and X denote standard group and test group, respectively. Φ is the fluorescence quantum yield, Grad is the gradient from the plot of integrated fluorescence intensity versus absorbance, and η is the refractive index of the solvent. In order to minimize the re-absorption effects, absorbance in the 10-mm fluorescence cuvette should never exceed 0.1 at the excitation wavelength.

Cell viability assay

The cytotoxicity of NCDs was evaluated on A549 cells using the MTS assay according to the protocol provided by the manufacturer (CellTiter Aqueous One Solution cell proliferation Assay kit from Promega). Briefly, A549 cells were seeded in a 96-well plate at a density of 3×10^3 cells/well and incubated for 24 h at 37 °C and 5 % CO_2, and then the growth medium was replaced with DMEM medium containing different concentrations of NCDs. Each sample was prepared in triplicates. After incubation for 24 h, 20 μL MTS solution was added to each well and incubated for 3 h at 37 °C under 5 % CO_2. The absorbance of each well was measured at 490 nm using Synergy HT Multi-Mode Microplate Reader (Bio Tek, USA). Non-treated cells (in DMEM) were used as control, and the relative cell viability (mean ± SD, n = 3) was expressed as Abs-sample/Abs-control × 100 %.

Cell imaging

A549 cells were chosen to demonstrate the feasibility of NCDs for the cell imaging. For fluorescent images, three different kinds of cells were seeded in a 24-well plate containing 15-mm-diameter glass cover-slips, in culture medium containing 10 % FBS incubated for 24 h at 37 °C and 5 % CO_2. The NCDs probes containing medium were then added to the cells at a concentration of 100 μg/ml. Cells were incubated at 37 °C under 5 % CO_2 for 6 h. After washing, confocal laser scanning fluorescence microscopy (Zeiss LSM-710) was used to observe the fluorescence in the cells with different wavelengths laser to excite the NCDs.

Results and discussion

The successful preparation of NCDs was carried out using citric acid as the carbon source and ammonium acetate as the surface passivation agent (Scheme 1). A simple microwave-assisted pyrolysis reaction formed the NCDs through dehydration, polymerization, aromatization, and surface passivation processes. A certain concentration of serine in the raw solution, which is critical to the degree of carbonization, was necessary to enhance the NCD formation.

Optimization of NCD synthesis conditions

To prepare fluorescent NCDs with optimized properties, the effects of the microwave irradiation time and concentration of surface passivation agent on the PL of NCDs were investigated. The PL intensity of the reaction solution initially increased with increasing irradiation time (Fig. 1a). In addition, a short irradiation time did not produce enough Joule heating for precursor dehydration and carbonization to occur, which was the reason that no PL was observed for less than 2 min of irradiation. The PL intensity of the reaction solution reached the maximum observed value after 6 min of irradiation, which was similar to that reported in the literature (Tan et al. 2013). When the irradiation time exceeded 6 min, the PL intensity became relatively weak, and the NCDs might form larger particles.

The appropriate amount of surface passivation was also essential for the NCDs to have the optimum PL intensity. Figure 1b shows the influence of ammonium

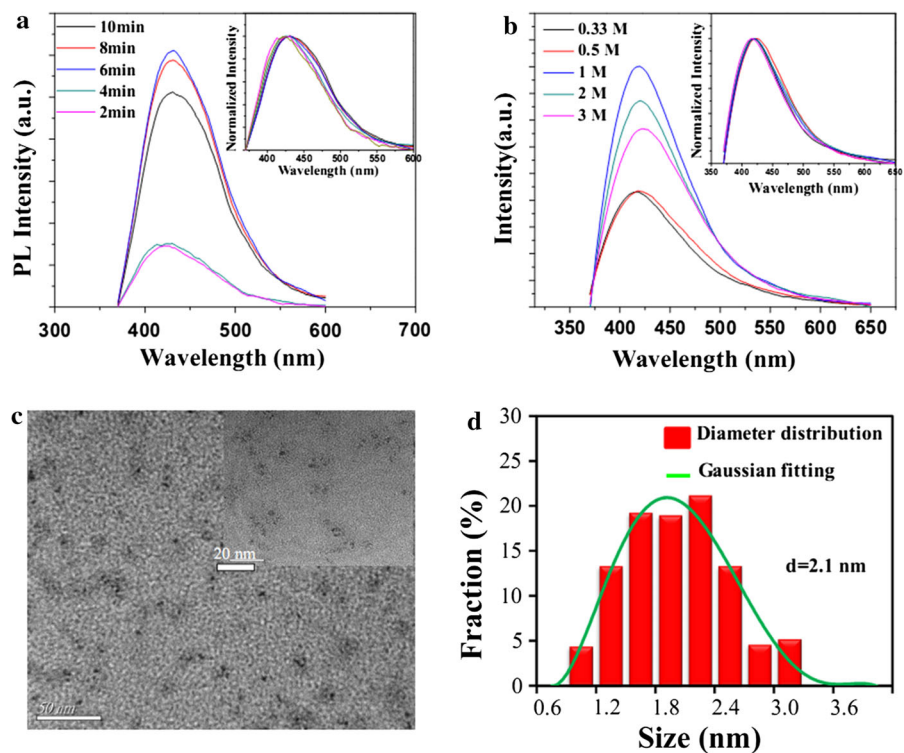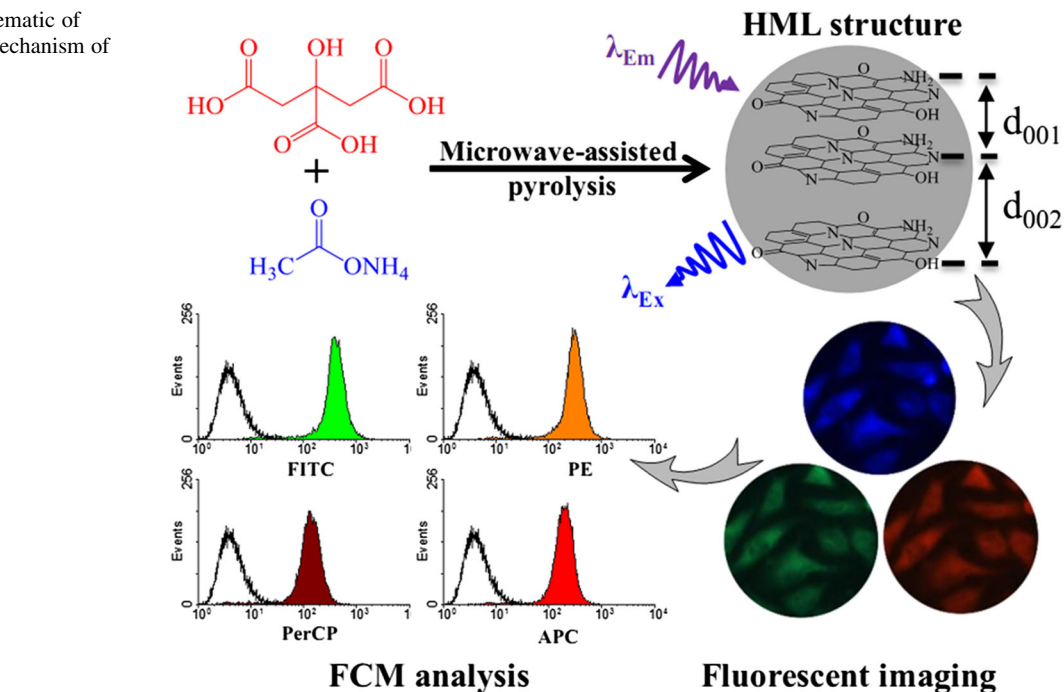**Scheme 1** Schematic of the formation mechanism of NCDs

Fig. 1 Preparation and characterization of NCDs. **a, b** PL spectra of NCDs prepared with different microwave pyrolysis time periods and ammonium acetate concentrations, respectively. The two *insets* are normalized PL spectra. **c** Low and high (*inset*) magnification TEM images. **d** The diameter distribution of prepared NCDs

acetate concentration on the PL intensity of the NCDs. The PL intensity increases with increasing ammonium acetate concentration, with the maximum PL intensity achieved, when 1 M of ammonium acetate was added to the precursor solution. The correct amount of ammonium acetate accelerates the dehydration process and the formation of NCDs. However, too much ammonium acetate dilutes the citric acid concentration, which results in incomplete reactions, and so the PL intensity decreases when the concentration of ammonium acetate is greater than 1 M. In the following sections, all samples used for characterization were synthesized with 1.9 g of citric acid, 0.77 g of ammonium acetate, and 6 min of microwave pyrolysis, unless specifically stated otherwise.

Characterization of NCDs

The morphology of the as-prepared NCDs was characterized by transmission electron microscopy (TEM) (Fig. 1c). We can see that the NCDs are discrete quasi-spheres in shape and relatively uniform in size. As shown in Fig. 1d, the distribution of NCD diameters conforms to a Gaussian curve. The average size of the NCDs was approximately 2.1 nm, as determined by the statistical analysis of more than one hundred particles using Image J software.

The optical properties of the NCDs were characterized with UV/vis and PL spectroscopy. The absorption spectrum (Fig. 2a) shows a strong absorption peak at 340 nm, which was ascribed to the n–π* transition of C=O. The aqueous solution of NCDs was pale yellow and transparent in daylight, but changed to a bright blue under UV excitation (inset, Fig. 2a). As shown in Fig. 2b, the NCDs have multicolor fluorescent emissions depending on the excitation wavelength used. When the excitation wavelength changes from 320 to 410 nm, the maximum emission peak position also shifts to a longer wavelength, from 430 to 480 nm (a red-shift of 50 nm). As the peak position of maximum emission changes, the PL intensity decreases greatly, showing the clear dependence of emission wavelength/intensity on the excitation wavelength. The full width at half maximum (FWHM) with an excitation of 350 nm is only 100 nm, which further confirms the narrow size distribution of the as-prepared NCDs. In addition, the aqueous solution of NCDs was a long-term homogeneous phase without any noticeable precipitation at room temperature. To verify the dispersibility, a beam of red light was used to illuminate the NCD aqueous solution. The Tyndall effect was clearly observed, as can be seen in Fig. 2c. The overall results illustrate that the prepared NCDs exhibit favorable fluorescent properties and good dispersibility in aqueous solutions.

To gain insight into the formation mechanism, the structure and chemical composition of the NCDs were investigated with X-ray diffraction (XRD) and FTIR spectroscopy, respectively. As shown in the FTIR spectrum (Fig. 2d), the broad characteristic peak of –OH at 3,430 cm^{-1}, the strong absorption peak of C=O at 1,770 cm^{-1}, and the stretching vibration peaks of C–O at 1,180 and 830 cm^{-1} are present. This is evidence for the presence of plentiful carboxylic acid and other oxygen-containing functional groups on the surface of the NCDs, which endows them with high water solubility. The stretching vibration peaks of N–H at 1,380 and 3,430 cm^{-1} are the evidence of the existence of amino-containing functional groups. These results indicate that there are many functional groups located on the surface of NCDs, mainly composed of amino, carbonyl, carboxylate, and hydroxyl groups. The presence of these functional groups gives the NCDs good solubility and improved fluorescent properties, which has been reported by others (Dong et al. 2013; Li et al. 2014; Ding et al. 2014; Xu et al. 2013; Zhang et al. 2013a).

Many studies have demonstrated that carbon dots have poor crystallinity, which is similar to a graphite-like phase structure (Zhang et al. 2012, 2013b; Nie et al. 2014). In this work, the phase structure of the NCDs was investigated with XRD, and graphite oxide (GO) powder was used as the control. As can be seen in Fig. 3, three diffraction peaks are clearly visible in the GO diffraction pattern, which correspond to the characteristic peaks of GO. The main peak around $2\theta = 12.04°$ in the NCD pattern is similar to the typical diffraction peak ($2\theta = 10.6°$, 001 plane) of GO. The d_{001} lattice spacing of the NCDs was determined to be 0.73 nm from the Bragg formula (as shown in Fig. 3), which is a smaller spacing than GO's spacing of 0.85 nm. We propose that the upward shift in peak position is caused by a decrease in the spacing between sp^3 layers. The two diffraction peaks around 29.6° and 42.1° in the NCD pattern correspond to the {002} and {100} planes of the graphitic framework, respectively. Compared to the ordered crystal structure of graphite (002 planes, $2\theta = 26.5$),
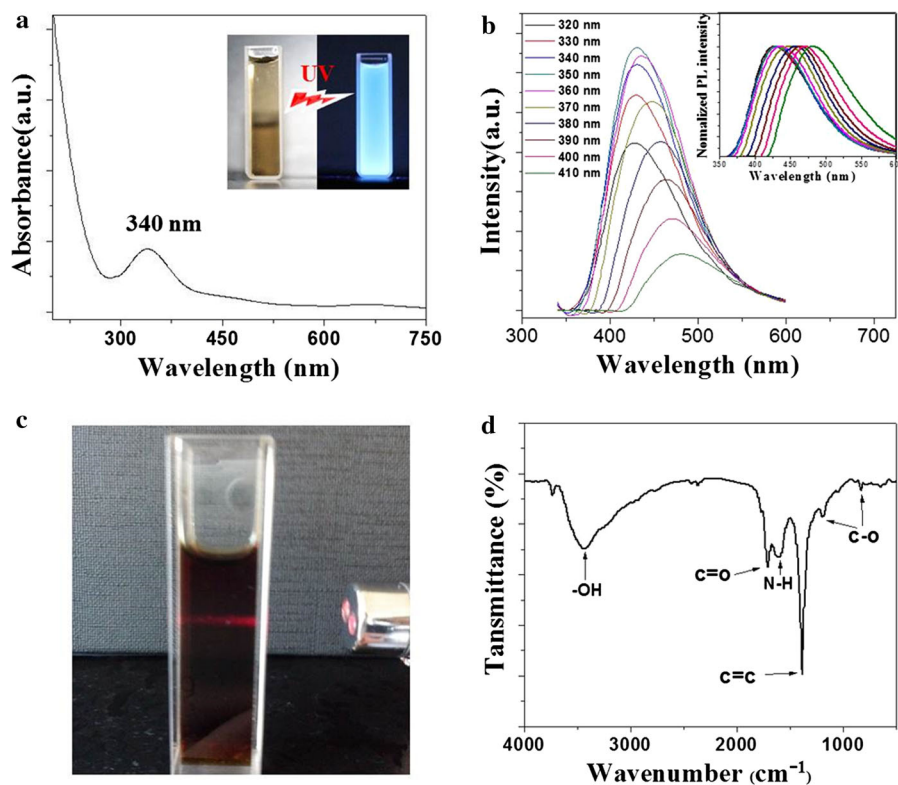
Fig. 2 **a**, **b** UV–vis absorbance and photoluminescence emission spectra of the NCDs, respectively. The *inset* of **a** shows a diluted aqueous solution containing the as-prepared NCDs. The PL emission spectra show the results of using progressively longer excitation wavelengths, from 320 to 410 nm in 10-nm increments. In the *inset* of **b**, the emission intensities are normalized. **c** The Tyndall effect exhibited by the NCDs in aqueous solution. **d** The FTIR spectrum of the NCDs

the broad diffraction peak of NCDs around 29.6° ($d_{002} = 0.3$ nm) was attributed to highly disordered carbon and a decrease in the sp^2 (C–C) layer spacing during the carbonization process. The shoulder peak at $2\theta = 42.5°$ ($d_{100} = 0.212$ nm) is attributed to in-plane diffraction from the graphene-like structure of the NCDs, which corresponds to the {100} plane of graphite. During the carbonization process, many functional groups, such as hydroxyl, carbonyl, epoxy, and amino groups, were bonded to the edges of the basal plane of the crystal structure, inducing a decrease in the graphite interlayer spacing. The above results clearly reveal that the prepared NCDs have poor crystallinity as a consequence of possessing a heterogeneous multi-layered structure, which is closer to the GO phase structure than the graphite structure.

The formation process of NCDs by microwave-assisted pyrolysis is extremely complicated, and a clear mechanism is still unknown (Yang et al. 2013; Huang et al. 2014; Qian et al. 2014). A plausible mechanism for the formation of NCDs may be as follows (Scheme 1). During the initial microwave pyrolysis stage, the dehydration and polymerization of citric acid and ammonium acetate gives rise to nitrogenous polymers. With time, the intermediates are condensed to form amorphous and crystalline phases, which is consistent with the XRD patterns. As the aromatization and carbonization of the phases progresses, NCDs are finally formed. It is worth mentioning that this process gives rise to hydrophilic functional groups (e.g., hydroxyl, amino, carbonyl, and carboxyl groups). Acting as a self-passivating layer, these functional groups endow the NCDs with excellent solubility in water, as well as the optimum photoluminescence properties.

Applications in biomedicine

The feasibility of synthesized NCDs as multifunctional probes in biomedical applications was evaluated. The
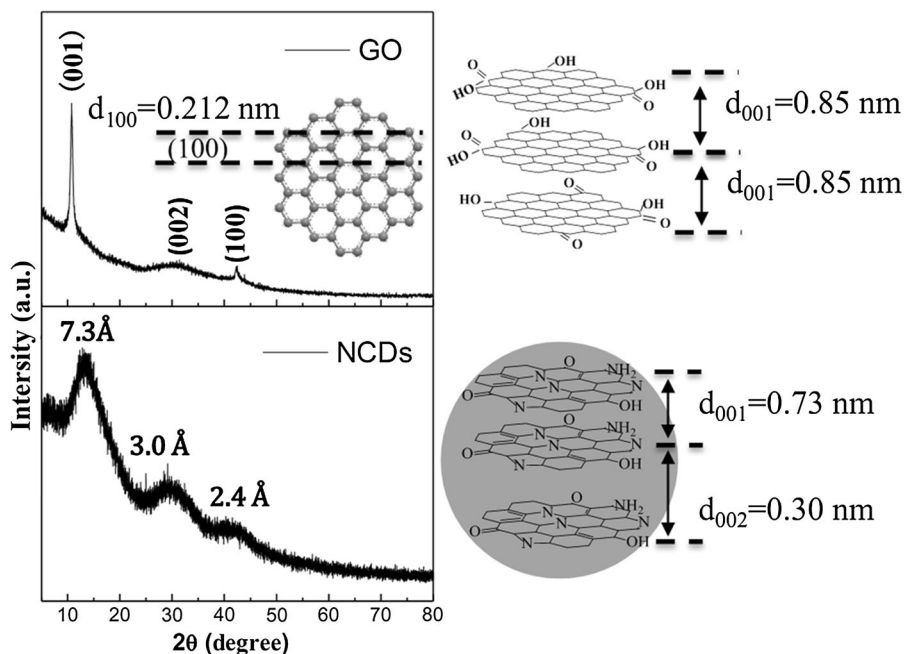
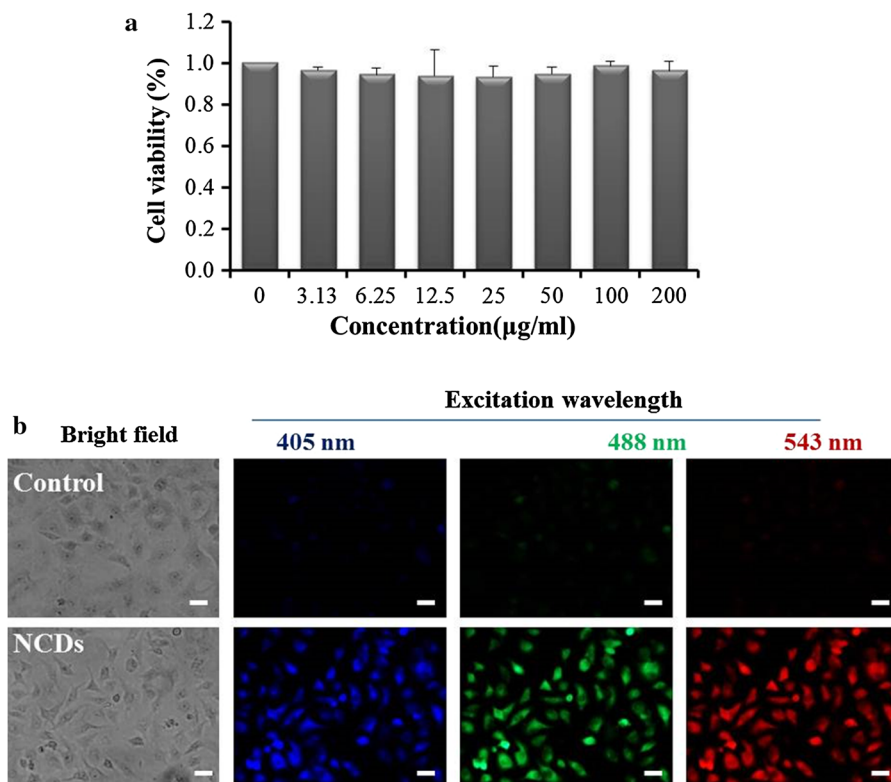**Fig. 3** The XRD patterns of NCDs and graphite oxide (GO)

Fig. 4 a Effect of NCDs on the viability of A549 cells using the MTS assay. **b** Laser scanning confocal microscopy images of A549 cells stained with NCDs exposed to 405, 488, and 543 nm excitation wavelengths. *Scale bars* = 50 μm

Fig. 5 a The two-channel (FL1 and FL2) dot plots of A549 cells labeled with NCDs. **b** The single-color histograms of A549 cells labeled with NCDs measured with four different channels
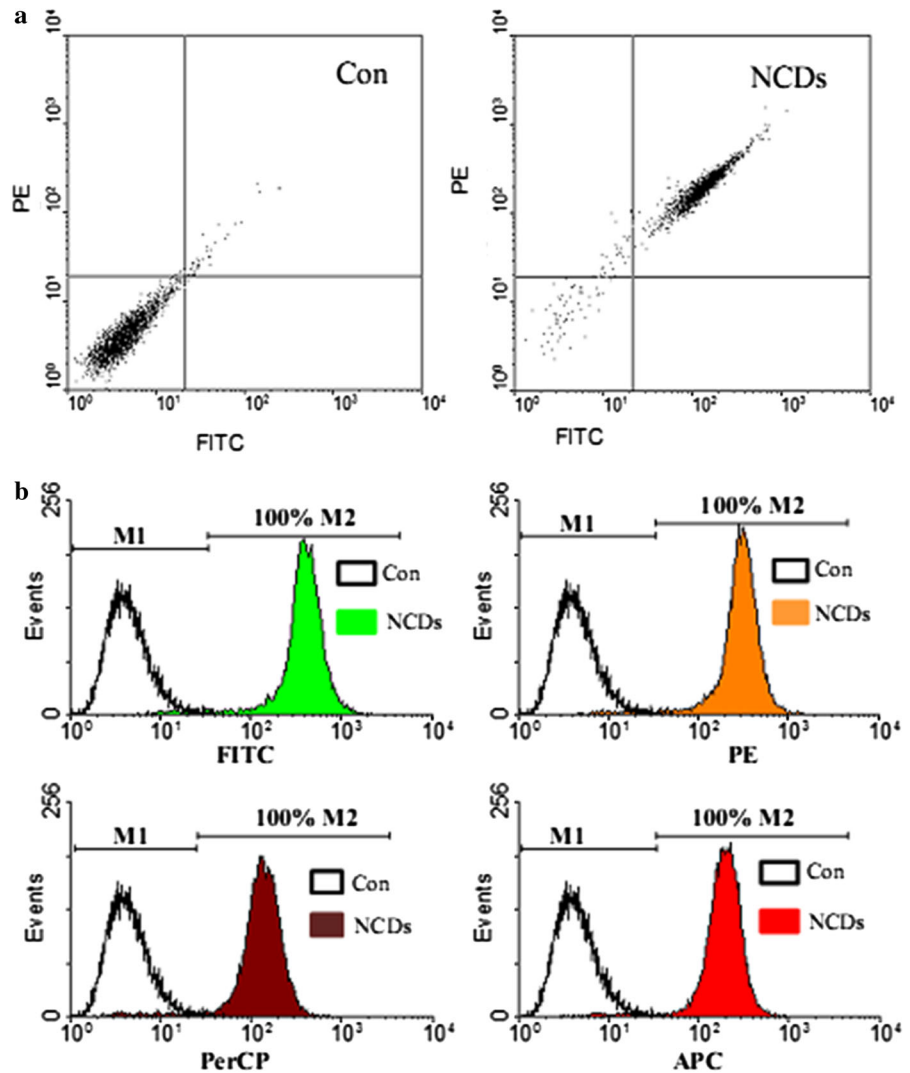
inherent cytotoxicity of NCDs was assessed in human lung adenocarcinoma A549 cells with an MTT assay. The A549 cell viabilities were determined after being exposed to different concentrations of NCDs for 24 h. Figure 4a shows that the NCDs exhibit very low toxicity, with cell viabilities of approximately 98.4 % for NCD concentrations less than 100 μg/ml. When the concentration of NCDs was increased to 200 μg/ml, the cell viability dropped to 96.2 %.

The potential application of NCDs in biomedicine was evaluated through laser scanning confocal microscopy and flow cytometry. A549 cells were cultured in a medium containing 100 μg/ml of NCDs for 6 h and then washed to remove free NCDs. As fluorescent probes, the excitation-dependent PL of synthesized NCDs gave rise to several visible consequences when imaged. As shown in Fig. 4b, the A549 cells became visible, appearing blue, green, and red under 405, 488, and 543 nm excitation wavelengths, respectively, while there was no sign of PL from the control groups. These results reveal that NCDs can easily and quickly pass through the cell membrane and be internalized into the cell. It is worth noting that the NCDs mainly resided in the cytosol, especially around the cell nucleus, while the PL of NCDs in the cell nucleus was very weak. We also found that the NCDs exhibited strong photostability, with no blink and little photobleaching observed.

Flow cytometry is one of the most useful biomedical techniques and is widely applied in biomedical fields, including disease diagnosis, cell sorting, and tumor detection. Developing new and efficient probes is essential for improving the accuracy and effectiveness of flow cytometry in clinical applications. In this study, we tested NCDs as potential multifunctional probes for flow cytometry. Compared with control groups, the two-channel plots (FL1 and FL2) show that 100 % of the living cells were labeled with NCDs (Fig. 5a). As shown in Fig. 5b, the four single-color histograms also indicate that the number of labeled cells was 100 %. The advantage of multi-channel detection is that different channels can verify each other, which can remove false-positive results and greatly improve the accuracy in practical applications. These results validate NCDs as multifunctional probes that can be detected by flow cytometry using four different channels simultaneously. Based on the above information, we propose that NCDs are ideal multifunctional platforms for biomedical applications.

Conclusions

In summary, we prepared highly fluorescent NCDs with a heterogeneous multi-layered phase structure and broadened their applicability to biomedical fields. The nitrogen-containing ammonium acetate used as the surface passivation agent can improve the PL properties of NCDs during the microwave irradiation reaction process. The various functional groups located at the surface of the NCDs endowed them with the hydrophilicity and photostability required for biomedical applications. These discrete quasi-spherical NCDs exhibited strong and tunable PL properties that are dependent on the excitation wavelength. The resultant NCDs had low cytotoxicity and were easily and quickly internalized into cytoplasm, with strong fluorescent signals emitted. Furthermore, NCDs acting as fluorescent agents were applied to flow cytometry analysis and showed excellent efficiency and accuracy. In view of these merits, these newly developed NCDs when used as multifunctional fluorescent agents have great potential applicability to biomedical research.

References

Baker SN, Baker GA (2010) Luminescent carbon nanodots: emergent nanolights. Angew Chem Int Ed Engl 49: 6726–6744

Cao L, Wang X, Meziani MJ, Lu FS, Wang HF, Luo PG, Lin Yi, Harruff BA, Veca M, Murray D, Xie SY, Sun YP (2007) Carbon dots for multiphoton bioimaging. J Am Chem Soc 129:11318–11319

Ding H, Zhang P, Wang T, Kong J, Xiong H (2014) Nitrogen-doped carbon dots derived from polyvinyl pyrrolidone and their multicolor cell imaging. Nanotechnology 25:205604

Dong Y, Pang H, Yang H, Guo C, Shao J, Chi Y, Li CM, Yu T (2013) Carbon-based dots co-doped with nitrogen and sulfur for high quantum yield and excitation-independent emission. Angew Chem Int Ed Engl 52:7800–7804

Du F, Li J, Hua Y, Zhang M, Zhou Z, Yuan J, Wang J, Peng W, Zhang L, Xia S, Wang D, Yang S, Xu W, Gong A, Shao Q (2014a) Multicolor nitrogen-doped carbon dots for live cell imaging. J Biomed Nanotechnol

Du FY, Zhang MM, Li X, Li JN, Jiang XY, Zhang LR, Hua Y, Shao GB, Jin J, Shao QS, Zhou M, Gong AH (2014b) Economical and green synthesis of bagasse-derived fluorescent carbon dots for biomedical applications. Nanotechnology 25:315702

Guo X, Wang CF, Yu ZY, Chen L, Chen S (2012) Facile access to versatile fluorescent carbon dots toward light-emitting diodes. Chem Commun 48:2692–2694

Han B, Wang W, Wu H, Fang F, Wang N, Zhang X, Xu S (2012) Polyethyleneimine modified fluorescent carbon dots and their application in cell labeling. Colloids Surf B Biointerfaces 100:209–214

Huang Y, Zhou X, Zhou R, Zhang H, Kang K, Zhao M, Peng Y, Wang Q, Zhang H (2014) One-pot synthesis of highly luminescent carbon quantum dots and their nontoxic ingestion by zebrafish for in vivo imaging. Chemistry 20:1–10

Jahan S, Mansoor F, Naz S, Lei JP, Kanwal S (2013) Oxidative synthesis of highly fluorescent boron/nitrogen co-doped carbon nanodots enabling detection of photosensitizer and carcinogenic dye. Anal Chem 85:10232–10239

Jiang F, Chen DQ, Li RM, Wang YC, Zhang GQ, Li SM, Zheng JP, Huang NY, Gu Y, Wang CR, Shu CY (2013) Eco-friendly synthesis of size-controllable amine-functionalized graphene quantum dots with antimycoplasma properties. Nanoscale 5:1137–1142

Lai TT, Zheng EH, Chen LX, Wang XY, Kong LC, You CP, Ruan YM, Weng XX (2013) Hybrid carbon source for producing nitrogen-doped polymer nanodots: one-pot hydrothermal synthesis, fluorescence enhancement and highly selective detection of Fe(III). Nanoscale 5: 8015–8021

Li HT, He XD, Kang ZH, Hui H, Liu Y, Liu JL, Lian SY, Tsang CH, Yang XB, Lee ST (2010) Water-soluble fluorescent carbon quantum dots and photocatalyst design. Angew Chem Int Ed Engl 49:4430–4434

Li N, Liang X, Wang L, Li Z, Li P, Zhu Y, Song J (2012) Biodistribution study of carbogenic dots in cells and in vivo for optical imaging. J Nanopart Res 14(10):1–9

Li W, Zhang Zh, Kong B, Feng SS, Wang JX, Wang LZ, Yang JP, Zhang F, Wu PY, Zhao DY (2013) Simple and green synthesis of nitrogen-doped photoluminescent carbonaceous nanospheres for bioimaging. Angew Chem Int Ed Engl 52:8151–8155

Li X, Zhang S, Kulinich SA, Liu Y, Zeng H (2014) Engineering surface states of carbon dots to achieve controllable luminescence for solid-luminescent composites and sensitive Be(2+) detection. Sci Rep 4:4976

Liong M, Hoang AN, Chung J, Gural N, Ford CB, Min C, Shah RR, Ahmad R, Marta FS, Fortune SM, Toner M, Hakho Lee, Weissleder R (2013) Magnetic barcode assay for genetic detection of pathogens. Nat Commun 4:1752

Nie H, Li M, Li Q, Liang S, Tan Y, Sheng L, Shi W, Zhang S (2014) Carbon dots with continuously tunable full-color emission and their application in ratiometric pH sensing. Chem Mater 26:3104–3112

Qian J, Chen J, Ruan S, Shen S, He Q, Jiang X, Zhu J, Gao H (2014) Preparation and biological evaluation of photoluminescent carbonaceous nanospheres. J Colloid Interface Sci 429:77–82

Sahu S, Behera B, Maiti TK, Mohapatra S (2012) Simple one-step synthesis of highly luminescent carbon dots from orange juice: application as excellent bio-imaging agents. Chem Commun 48:8835–8837

Stefanakis D, Philippidis A, Sygellou L, Filippidis G, Ghanotakis D, Anglos D (2014) Synthesis of fluorescent carbon dots by a microwave heating process: structural characterization and cell imaging applications. J Nanopart Res 16(10):1–10

Tan M, Zhang L, Tang R, Song X, Li Y, Wu H, Wang Y, Lv G, Liu W, Ma X (2013) Enhanced photoluminescence and characterization of multicolor carbon dots using plant soot as a carbon source. Talanta 115:950–956

Wang J, Kroll P (2012) Structural, electronic and optical properties of sic quantum dots. J Nano Res 18:77–87

Wang J, Wang CF, Chen S (2012) Amphiphilic egg-derived carbon dots: rapid plasma fabrication, pyrolysis process, and multicolor printing patterns. Chen. Angew Chem Int Ed Engl 51:9297–9301

Wang QL, Huang XX, Long YJ, Wang XL, Zhang HJ, Zhu R, Liang LP, Teng P, Zheng HZ (2013) Hollow luminescent carbon dots for drug delivery. Carbon 59:192–199

Wei WL, Xu C, Wu L, Wang J, Ren JS, Qu XG (2014) Non-enzymatic-browning reaction: a versatile route for production of nitrogen-doped carbon dots with tunable multicolor luminescent display. Sci Rep 4:3564

Xu X, Ray R, Gu Y, Ploehn HJ, Gearheart L, Raker K, Scrivens WA (2004) Electrophoretic analysis and purification of fluorescent single-walled carbon nanotube fragments. J Am Chem Soc 126:12736–12737

Xu Y, Wu M, Liu Y, Feng X, Yin X, He X, Zhang Y (2013) Nitrogen-doped carbon dots: a facile and general preparation method, photoluminescence investigation, and imaging applications. Chemistry 19:2276–2283

Yang Z, Xu M, Liu Y, He F, Gao F, Su Y, Wei H, Zhang Y (2013) Nitrogen-doped, carbon-rich, highly photoluminescent carbon dots from ammonium citrate. Nanoscale 6:1890

Zhai X, Zhang P, Liu C, Bai T, Li W, Dai L (2012) Highly luminescent carbon nanodots by microwave-assisted pyrolysis. Chem Commun 48:7955–7957

Zhang RZ, Chen W (2014) Nitrogen-doped carbon quantum dots: facile synthesis and application as a "turn-off" fluorescent probe for detection of Hg^{2+} ions. Biosens Bioelectron 55:83–90

Zhang Z, Hao J, Zhang J, Zhang B, Tang J (2012) Protein as the source for synthesizing fluorescent carbon dots by a one-pot hydrothermal route. RSC Adv 2:8599–8601

Zhang R, Liu YB, Sun SQ (2013a) Preparation of highly luminescent and biocompatible carbon dots using a new extraction method. J Nanopart Res 15:2010

Zhang X, Wang S, Zhu C, Liu M, Ji Y, Feng L, Tao L, Wei Y (2013b) Carbon-dots derived from nanodiamond: photoluminescence tunable nanoparticles for cell imaging. J Colloid Interface Sci 397:39–44

Zhu H, Wang XL, Li YL, Wang ZJ, Yang F, Yang XR (2009) Microwave synthesis of fluorescent carbon nanoparticles with electrochemiluminescence properties. Chem Commun 34:5118–5120

Zhu CZ, Zhai JF, Dong SJ (2012) Bifunctional fluorescent carbon nanodots: green synthesis via soy milk and application as metal-free electrocatalysts for oxygen reduction. Chem Commun 48:9367–9369